

# An Operationally Simple Method for Separating the Rare-Earth Elements Neodymium and Dysprosium\*\*

Justin A. Bogart, Connor A. Lippincott, Patrick J. Carroll, and Eric J. Schelter\*

**Abstract:** Rare-earth metals are critical components of electronic materials and permanent magnets. Recycling of consumer materials is a promising new source of rare earths. To incentivize recycling there is a clear need for simple methods for targeted separations of mixtures of rare-earth metal salts. Metal complexes of a tripodal nitroxide ligand  $[(2\text{-}^t\text{BuNO})\text{C}_6\text{H}_4\text{CH}_2]_3\text{N}]^{3-}$  ( $\text{TriNOx}^{3-}$ ), feature a size-sensitive aperture formed of its three  $\eta^2\text{-(N,O)}$  ligand arms. Exposure of metal cations in the aperture induces a self-associative equilibrium comprising  $[\text{M}(\text{TriNOx})\text{thf}]/[\text{M}(\text{TriNOx})]_2$  ( $\text{M}$  = rare-earth metal). Differences in the equilibrium constants ( $K_{\text{eq}}$ ) for early and late metals enables simple Nd/Dy separations through leaching with a separation ratio  $S_{\text{Nd/Dy}} = 359$ .

The rare-earth elements (M), La–Lu, Y, and Sc, are key components of vital materials with diverse applications in electric motors, phosphors, nickel–metal–hydride batteries, and catalysts, among others.<sup>[1]</sup> Their broad, and in many cases irreplaceable, uses result from unique properties arising from their 4f valence electron shell. Neodymium (Nd), typically mixed with praseodymium (Pr), is a key component of sintered neodymium magnets (or “neo magnets”;  $\text{Nd}_2\text{Fe}_{14}\text{B}$ ), which have the highest-energy product (52 MGOe) among commercialized permanent magnets.<sup>[2]</sup> Terbium (Tb) and dysprosium (Dy) are also key components of this material which increase its intrinsic coercivity.<sup>[3]</sup> High-performance neo magnets include up to 9% Dy by total magnet weight.<sup>[4]</sup> The U.S. Department of Energy has categorized dysprosium and neodymium as “critical materials” because of their supply problems and importance to technology.<sup>[5]</sup>

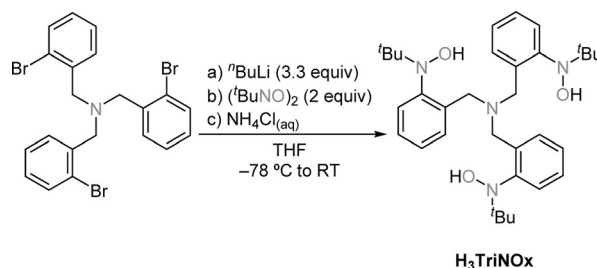
A potential new supply stream of neodymium and dysprosium is end-of-life magnet recycling. In 2007, global in-use stocks for rare-earth metals in neo magnets were estimated to be 62.6 Gg of Nd, 15.7 Gg of Pr and Dy, and 3.1 Gg of Tb.<sup>[6]</sup> In 2011, however, less than 1% of rare-earth metals were recycled.<sup>[4]</sup> A recent life-cycle assessment sug-

gested that end-of-life product recycling is a viable alternative to the mining of rare-earth metals.<sup>[7]</sup> Recycling processes have been reported for the isolation of mixtures of rare-earth metals from dismantled magnetic materials<sup>[4,8]</sup> and significant advances have been made toward processing magnets to produce rare-earth concentrates.<sup>[9]</sup> However, the varying blends of Dy, Tb, Nd, and Pr necessitate separations of the rare earths for reblending into new sintered magnets in the highest-value recycling schemes.

Rare-earth metals are separated commercially using a Rhône–Poulenc liquid–liquid extraction process (LLE), an energy-, time- and solvent-intensive process that exploits differences in binding constants of the metals to organic extractants.<sup>[10]</sup> Recent fundamental studies have worked to enhance the selectivity for one type of rare-earth metal cation over another, based on ionic size, through molecular self-assembly of helical  $\text{Ln}_2\text{L}_3$  dimers,<sup>[14]</sup> or with the use of lanthanide-based metal–organic frameworks for fractional crystallization.<sup>[15]</sup> It is of interest to develop simple and direct chemical methods for efficient separations of early and late rare-earth metals, namely dysprosium and neodymium, to incentivize recycling from their primary consumer use in magnets.

Herein, we report rare-earth-metal coordination compounds of  $[(2\text{-}^t\text{BuNO})\text{C}_6\text{H}_4\text{CH}_2]_3\text{N}]^{3-}$  ( $\text{TriNOx}^{3-}$ ) that undergo a self-association (dimerization) equilibrium based on cation size. As a result of the relatively larger value of its self-association equilibrium constant, the Nd– $\text{TriNOx}$  system exhibits a 50-fold higher solubility than the Dy– $\text{TriNOx}$  system in benzene. Taken together, the solubility and self-association equilibria achieve a separation factor  $S_{\text{Nd/Dy}} = 359$  using simple solvent leaching, providing proof-of-concept for targeted separations of consumer materials.

To initiate the separation studies, the tripodal nitroxide ligand  $[(2\text{-}^t\text{BuNOH})\text{C}_6\text{H}_4\text{CH}_2]_3\text{N}]$ , tris(2-*tert*-butylhydroxyaminato)benzylamine ( $\text{H}_3\text{TriNOx}$ ), was synthesized in 70% yield by a lithium–halogen exchange reaction between tris-2-bromobenzylamine<sup>[16]</sup> and  $^t\text{BuLi}$  at  $-78^\circ\text{C}$ , followed by the addition of 2-methyl-2-nitrosopropane dimer (Scheme 1).



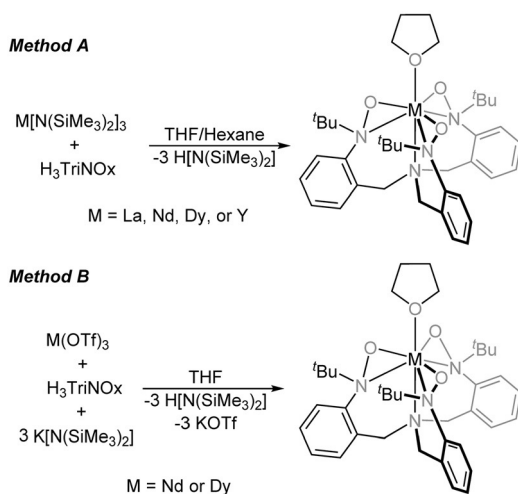
Scheme 1. Synthesis of the  $\text{H}_3\text{TriNOx}$  ligand.

[\*] J. A. Bogart, C. A. Lippincott, Dr. P. J. Carroll, Prof. E. J. Schelter  
Department of Chemistry  
University of Pennsylvania  
231 S. 34th St., Philadelphia, PA 19104 (USA)  
E-mail: schelter@sas.upenn.edu

[\*\*] E.J.S. acknowledges the U.S. Department of Energy, Office of Science, Early Career Research Program (Grant DE-SC0006518), the Research Corporation for Science Advancement (Cottrell Scholar Award to E.J.S.), and the University of Pennsylvania for financial support of this work. We thank Dr. Andrew J. Lewis for helpful discussions.

Supporting information for this article is available on the WWW under <http://dx.doi.org/10.1002/anie.201501659>.

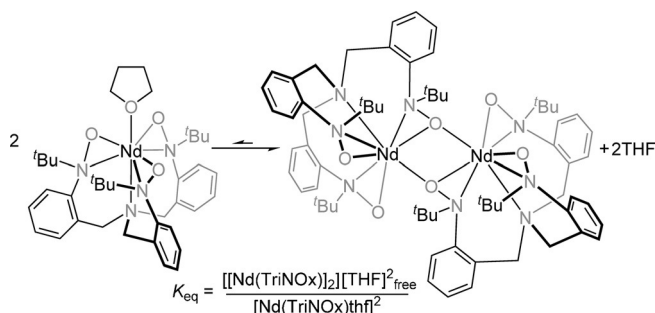
$\text{H}_3\text{TriNOx}$  was air stable in both the solid and solution states. Isostructural  $[\text{M}(\text{TriNOx})\text{thf}]$  compounds, where  $\text{M} = \text{La}$ ,  $\text{Nd}$ ,  $\text{Dy}$ , and  $\text{Y}$ , were formed through a simple protonolysis route between  $\text{H}_3\text{TriNOx}$  and their respective  $\text{M}^{\text{III}}[\text{N}(\text{SiMe}_3)_2]_3$  reagents (Scheme 2, method A). These compounds exhibited



**Scheme 2.** Methods A and B for the preparation of metal complexes  $[\text{M}(\text{TriNOx})\text{thf}]$ . OTf = trifluoromethanesulfonate.

only low solubility in THF (see below). The compounds could also be synthesized through an alternative, one-pot synthetic route starting from the  $\text{M}(\text{OTf})_3$  salts,  $\text{H}_3\text{TriNOx}$  (1 equiv), and  $\text{K}[\text{N}(\text{SiMe}_3)_2]$  (3 equiv) in THF (Scheme 2, method B). The structures of the  $[\text{M}(\text{TriNOx})\text{thf}]$  complexes revealed that each arm of the nitroxide ligand was coordinated  $\eta^2$ -( $\text{N},\text{O}$ ) to the rare-earth cations. This coordination mode provided a  $\text{C}_3$ -symmetric environment with an open site in the apical position, occupied by a THF molecule.

Analysis of the solution structures of  $[\text{M}(\text{TriNOx})\text{thf}]$  in  $\text{CD}_2\text{Cl}_2$  ( $\text{M} = \text{La}$  and  $\text{Nd}$ ) using  $^1\text{H}$  NMR spectroscopy revealed two species in solution in each case, consistent with the presence of  $[\text{M}(\text{TriNOx})\text{thf}]$  complexes and  $\text{C}_2$ -symmetric dimeric compounds (Scheme 3). The identities of the dimeric compounds were confirmed crystallographically (Figure 1) and the compounds were isolated in good yields by dissolving  $[\text{M}(\text{TriNOx})\text{thf}]$  ( $\text{M} = \text{La}$ ,  $\text{Nd}$ ) in toluene and removing the solvent under reduced pressure. The



**Scheme 3.** The equilibrium between monomeric  $[\text{M}(\text{TriNOx})\text{thf}]$  and dimeric  $[\text{M}(\text{TriNOx})]_2$ .

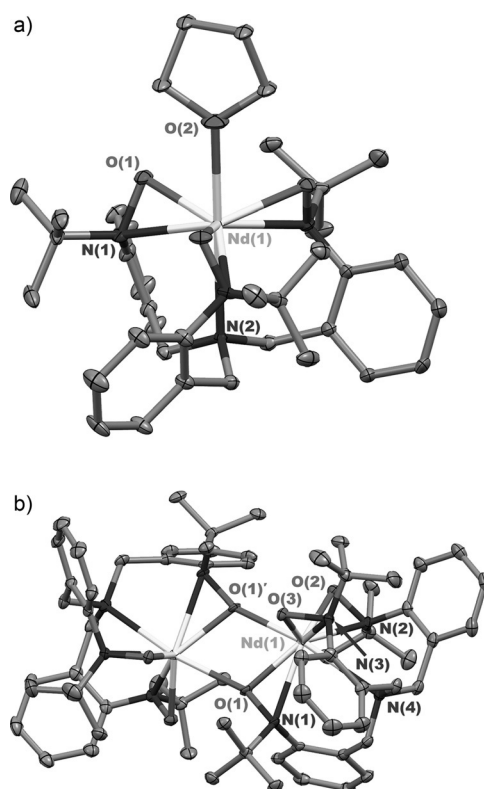


**Figure 1.** Crystal structures of a) the monomer  $[\text{Nd}(\text{TriNOx})\text{thf}]$  and b) the dimer  $[\text{Nd}(\text{TriNOx})]_2$ . Thermal ellipsoids are set at 30% probability.<sup>[17]</sup>

$[\text{M}(\text{TriNOx})]_2$  compounds could be converted back into the respective  $[\text{M}(\text{TriNOx})\text{thf}]$  congeners by addition of THF to their benzene, toluene, or methylene chloride solutions. In the cases of  $\text{M} = \text{Dy}$  or  $\text{Y}$ , dimers were not detected.

The existence of  $[\text{M}(\text{TriNOx})]_2$  dimers in solutions of  $\text{CH}_2\text{Cl}_2$  was also evident from solution-state electrochemistry experiments.  $[\text{La}(\text{TriNOx})\text{thf}]$  and  $[\text{Nd}(\text{TriNOx})\text{thf}]$  exhibited similar cyclic voltammograms that showed two overlapping, quasi-reversible ligand oxidation waves between 0 and  $-0.75$  V versus  $\text{Fc}/\text{Fc}^+$  (ferrocene/ferrocenium) followed by an irreversible oxidation feature at  $+0.4$  V. In contrast, the cyclic voltammograms of  $[\text{M}(\text{TriNOx})\text{thf}]$  ( $\text{M} = \text{Y}$  and  $\text{Dy}$ ) showed one quasi-reversible oxidation with  $E_{\text{pa}} = +0.2$  V and  $E_{\text{pc}} = -0.5$  V (see the Supporting Information).

The value of the equilibrium constant for the dimerization of  $[\text{Nd}(\text{TriNOx})\text{thf}]$  in benzene (Scheme 3) was determined using  $^1\text{H}$  NMR spectroscopy at RT. A solution of  $[\text{Nd}(\text{TriNOx})]_2$  in  $\text{C}_6\text{D}_6$  was titrated with THF and the equilibrium concentrations of  $[\text{Nd}(\text{TriNOx})]_2$  and  $[\text{Nd}(\text{TriNOx})\text{thf}]$  were measured at each point against an internal ferrocene standard (see the Supporting Information). These data yielded a value of  $K_{\text{eq}} = 2.4 \pm 0.2$ . Measurement of the equilibrium constant was also possible using hypersensitive  $^4\text{I}_{9/2} \rightarrow ^2\text{G}_{7/2}$ ,  $^4\text{G}_{5/2}$  4f–4f transitions for the Nd–TriNOx system. A spectrophotometric titration of the Nd dimer in benzene with THF revealed a clear isosbestic point at  $\lambda = 594.1$  nm and the data yielded an equilibrium constant of  $K_{\text{eq}} = 2.9 \pm 0.4$ , in good agreement with the results from the NMR titration.

We postulated that the attenuated tendency for dimerization with decreasing ionic radius was due to an effective closing of the (N,O)<sub>3</sub> aperture formed by the three η<sup>2</sup>-(N,O) arms of the TriNOx<sup>3-</sup> ligand. To quantify the decrease in aperture size, we determined the percent buried volume (% *V*<sub>bur</sub>) for [Nd(TriNOx)thf] and [Dy(TriNOx)thf].<sup>[18]</sup> Upon changing the metal from Nd to Dy, we calculated an increase in % *V*<sub>bur</sub> from 79.9 % to 81.3 %, respectively. We contend that this small, but significant, increase in the % *V*<sub>bur</sub> and the change in size of the (N,O)<sub>3</sub> molecular aperture is responsible for shifting the thermodynamic preference from dimer to monomer in the TriNOx system.

The preferential formation of dimeric structures from the larger cations La and Nd with the TriNOx<sup>3-</sup> ligand and monomeric ones from the smaller Dy and Y was promising for targeted separations of Nd and Dy. To test for the formation of mixed metal dimers, which would interfere with a clean separation, <sup>1</sup>H EXSY NMR spectroscopic experiments were performed on mixtures of [Nd(TriNOx)thf] and [Dy(TriNOx)thf] in CD<sub>2</sub>Cl<sub>2</sub>. No exchange was detected between Nd and Dy during these experiments. <sup>1</sup>H EXSY NMR spectroscopic experiments were also performed on mixtures of [Nd(TriNOx)thf] and [Y(TriNOx)thf], a diamagnetic analogue of the [Dy(TriNOx)thf] complex, to allow for longer delay times; no cation exchange was detected in the Nd/Y experiments (see the Supporting Information).

The absence of mixed-metal dimer formation prompted us to determine conditions where the dimerization of [Nd(TriNOx)thf] could be exploited for solubility differences between the Nd and Dy species. Significantly different solubilities were found for the [Nd(TriNOx)thf] and [Dy(TriNOx)thf] complexes in benzene. These solubilities were quantified by <sup>1</sup>H NMR spectroscopy, where saturated C<sub>6</sub>D<sub>6</sub> solutions of the complexes were prepared and measured against a ferrocene internal standard. The solubility values of 60 mmol L<sup>-1</sup> and 1.2 mmol L<sup>-1</sup> determined for the Nd and Dy species, respectively, suggested that benzene could be used to effectively separate these ions.<sup>[19]</sup>

To test the feasibility of a separations method based on the [Nd(TriNOx)thf]/[Nd(TriNOx)]<sub>2</sub> equilibrium, 50:50 mixtures of [Nd(TriNOx)thf] and [Dy(TriNOx)thf] were isolated in 90 % yield by reacting equimolar mixtures of Nd(OTf)<sub>3</sub> and Dy(OTf)<sub>3</sub> with H<sub>3</sub>TriNOx (2 equiv) and K[N(SiMe<sub>3</sub>)<sub>2</sub>] (6 equiv) in THF (Figure 2a). The ratio of rare-earth elements in the prepared mixture was confirmed by <sup>1</sup>H NMR spectroscopy. The [Nd(TriNOx)thf] was selectively leached into minimal benzene leaving a solid residue enriched with [Dy(TriNOx)thf]. The ratios of rare earths in the final filtrate and solid phases were determined by <sup>1</sup>H NMR spectroscopy and inductively coupled plasma optical emission spectroscopy (ICP-OES).<sup>[20]</sup> Good agreement between the two methods was obtained. The ICP-OES data showed the filtrate was enriched to 95.37 % Nd while the solid was enriched to 94.56 % Dy (Figure 2b), providing a separation factor *S*<sub>Nd/Dy</sub> = 359.<sup>[13]</sup> Subsequent extractions with benzene to the isolated fractions improved the purities of both the filtrate and solid phases to 97.90 % Nd and 95.28 % Dy. The more benign solvent toluene was also used to achieve comparable separations of Nd and Dy, albeit with larger solvent volumes.

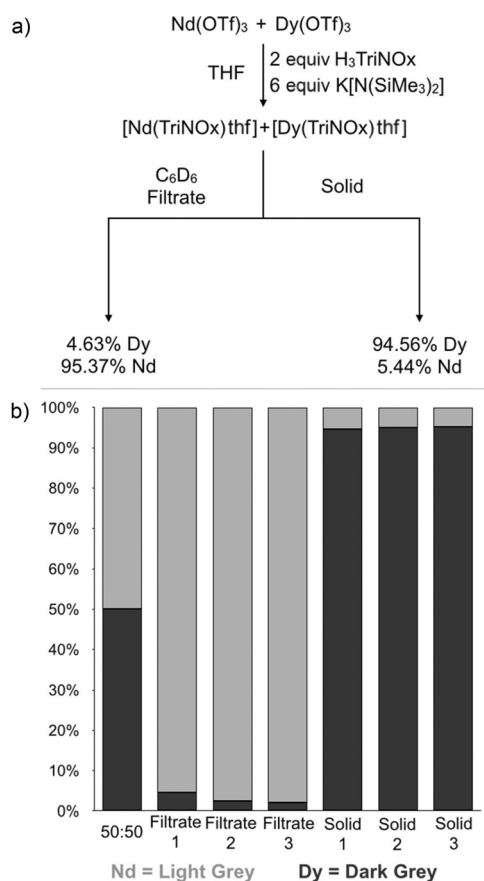


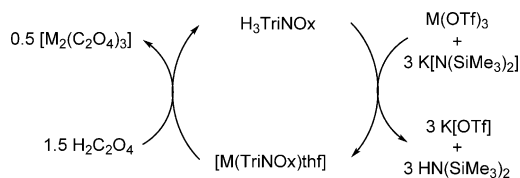
**Figure 2.** a) Schematic of the improved separation process of Nd and Dy and b) bar graph showing the enrichment in the rare-earth metal at each separation cycle.

The *S*<sub>Nd/Dy</sub> = 359 achieved for the M–TriNOx system compared favorably to that of 41.5 determined for the M<sup>III</sup>–HCl–HDEHP extraction method used industrially (HDEHP = di-(2-ethylhexyl)phosphoric acid), indicating an approximately 10-fold improvement in the separation of Nd and Dy.<sup>[11]</sup> It was also an approximately 1.5-fold improvement compared to the separation based on the M<sup>III</sup>–HNO<sub>3</sub>–Cyanex 302 system.<sup>[12]</sup>

A separation was also performed on a 75:25 mole ratio mixture of [Nd(TriNOx)thf] to [Dy(TriNOx)thf], a ratio that is used in Nd<sub>2</sub>Fe<sub>14</sub>B high-performance magnets. The filtrate phase was enriched to 97.6 % Nd and the solid phase was enriched to 95.2 % Dy as indicated by <sup>1</sup>H NMR spectroscopic analysis. These results were comparable to those obtained from the 50:50 mixtures.

Aqueous oxalic acid solutions (1.5 equiv) were added to pure samples of [Nd(TriNOx)thf] and [Dy(TriNOx)thf] in an effort to reclaim the TriNOx ligand. In both cases, pure H<sub>3</sub>TriNOx was extracted using chloroform (3 × 50 mL) in 87 % and 77 % recoveries, respectively. Based on these results, a complete synthetic cycle was performed, starting from the addition of THF solutions of H<sub>3</sub>TriNOx to mixtures of Nd/Dy(OTf)<sub>3</sub> salts and ending with the isolation of [M<sub>2</sub>(C<sub>2</sub>O<sub>4</sub>)<sub>3</sub>] (M = Nd, Dy) and the recovery of H<sub>3</sub>TriNOx (Scheme 4).

We have demonstrated an important proof-of-concept showing that differences in the self-association equilibria



**Scheme 4.** Representation of the recyclability of the ligand, leading to the isolation of  $[M_2(C_2O_4)_3]$  ( $M = Nd, Dy$ ) and the recovery of  $H_3TriNOx$ .

between Nd and Dy centers can be exploited for separation of these ions. Our results suggest that the use of coordination chemistry toward the realization of size-sensitive molecular apertures of N,O ligands could contribute to new methods for rare-earth-element separations. Such methods are advantageous for targeted separations because they are expected to eliminate the capital cost associated with mixer-settler equipment used in liquid-liquid extraction, making recycling of these critical materials more economically feasible. We are currently examining methods to improve upon this separation method using smaller volumes of more benign solvents and modified ligand systems.

**Keywords:** magnet recycling · metal separation · neodymium · N,O ligands · rare earths

**How to cite:** *Angew. Chem. Int. Ed.* **2015**, *54*, 8222–8225  
*Angew. Chem.* **2015**, *127*, 8340–8343

- [1] M. Humphries, *Rare Earth Elements: The Global Supply Chain*, Congressional Research Service, CRS Report R41347, Washington DC, **2013**, pp. 1–26.
- [2] a) D. Goll, H. Kronmüller, *Naturwissenschaften* **2000**, *87*, 423–438; b) O. Gutfleisch, M. A. Willard, E. Brück, C. H. Chen, S. G. Sankar, J. P. Liu, *Adv. Mater.* **2011**, *23*, 821–842.
- [3] M. Sagawa, S. Fujimura, H. Yamamoto, Y. Matsuura, K. Hiraga, *IEEE Trans. Magn.* **1984**, *20*, 1584–1589.
- [4] K. Binnemans, P. T. Jones, B. Blanpain, T. Van Gerven, Y. Yang, A. Walton, M. Buchert, *J. Clean Prod.* **2013**, *51*, 1–22.
- [5] U.S. Department of Energy, Critical Materials Strategy, Washington, DC, **2011**, pp. 1–191.

- [6] X. Du, T. E. Graedel, *J. Ind. Ecol.* **2011**, *15*, 836–843.
- [7] B. Sprecher, Y. Xiao, A. Walton, J. Speight, R. Harris, R. Kleijn, G. Visser, G. J. Kramer, *Environ. Sci. Technol.* **2014**, *48*, 3951–3958.
- [8] a) C. Sonich-Mullin, *Rare Earth Elements: A Review of Production, Processing, Recycling and Associated Issues*, Cincinatti, **2012**; b) D. Schüller, M. Buchert, R. Liu, S. Dittrich, C. Merz, *Study on Rare Earths and Their Recycling*, Darmstadt, **2011**; c) T. Elwert, D. Goldmann, F. Römer, *World Metall.-Erzmet.* **2013**, *66*, 209–219; d) T. Elwert, D. Goldmann, F. Römer, *World Metall.-Erzmet.* **2014**, *67*, 287–296.
- [9] T. Vander Hoogerstraete, B. Blanpain, T. Van Gerven, K. Binnemans, *RSC Adv.* **2014**, *4*, 64099–64111.
- [10] F. Xie, T. A. Zhang, D. Dreisinger, F. Doyle, *Miner. Eng.* **2014**, *56*, 10–28.
- [11] C. K. Gupta, N. Krishnamurthy in *Extractive Metallurgy of Rare Earths*, CRC, New York, **2005**, pp. 1–484.
- [12] M. Yuan, A. Luo, D. Li, *Acta Metall. Sin.* **1995**, *8*, 10–14.
- [13] The parameter  $S_{Nd/Dy}$  was calculated using the equation:  $S_{Nd/Dy} = (n_{Nd \text{ filtrate}}/n_{Nd \text{ solid}})/(n_{Dy \text{ filtrate}}/n_{Dy \text{ solid}}) = (n_{Nd \text{ filtrate}}/n_{Dy \text{ filtrate}})/(n_{Nd \text{ solid}}/n_{Dy \text{ solid}})$ .
- [14] A. M. Johnson, M. C. Young, X. Zhang, R. R. Julian, R. J. Hooley, *J. Am. Chem. Soc.* **2013**, *135*, 17723–17726.
- [15] X. Zhao, M. Wong, C. Mao, T. X. Trieu, J. Zhang, P. Feng, X. Bu, *J. Am. Chem. Soc.* **2014**, *136*, 12572–12575.
- [16] Q. Chen, C. Buss, V. Young, Jr., S. Fox, *J. Chem. Crystallogr.* **2005**, *35*, 177–181.
- [17] CCDC-1050572 ( $H_3TriNOx$ ), 1050573 ( $[Nd(TriNOx)thf]$ ), 1050574 ( $[Nd(TriNOx)]_2$ ), 1050575 ( $[Dy(TriNOx)thf]$ ), 1050576 ( $[La(TriNOx)thf]$ ), 1050577 ( $[La(TriNOx)]_2$ ), and 1050578 ( $[Y(TriNOx)thf]$ ) contain the supplementary crystallographic data for this paper. These data can be obtained free of charge from The Cambridge Crystallographic Data Centre via [www.ccdc.cam.ac.uk/data\\_request/cif](http://www.ccdc.cam.ac.uk/data_request/cif).
- [18] A. Poater, B. Cosenza, A. Correa, S. Giudice, F. Ragone, V. Scarano, L. Cavallo, *Eur. J. Inorg. Chem.* **2009**, 1759–1766.
- [19] J. A. Bogart, E. J. Schelter, Provisional Patent Disclosure, U.S. Application No. 62/030,227, **2014**.
- [20] G. L. Scheffler, F. R. S. Bentlin, D. Pozebon, *Br. J. Anal. Chem.* **2012**, *8*, 358–365.

Received: February 19, 2015

Revised: April 16, 2015

Published online: May 26, 2015